Integrated cross-scale derivative bounds for Wilson lattice gauge theory: closing the log-Sobolev gap

Lluis Eriksson
Independent Researcher
lluiseriksson@gmail.com

February 2026

Abstract

We prove integrated cross-scale derivative bounds that replace the unverified Assumption 5.4 of [6]. Combined with two explicit large-field inputs (Hypotheses 3.2 and 4.2) and the conditional inequalities of [7], this yields a uniform (volume-independent) log-Sobolev inequality for the Wilson lattice gauge measure at sufficiently weak coupling (large β). The key innovation is a decomposition into small-field and large-field contributions: the former is controlled by Balaban's polymer expansion, while the latter is handled by a pointwise gradient bound combined with exponential measure suppression. We provide a self-contained verification of the unconditional large-field tail mechanism for SU(2) in $d = 2$, together with numerical validation.

Contents

1 Introduction

1.1 Context and motivation

The construction of a rigorous non-perturbative framework for Yang–Mills theories on the lattice has been a central goal of mathematical physics since the foundational work of Wilson [0] and the analytical program of Balaban [1, 2, 3, 4]. A key milestone in this program is the establishment of *uniform functional inequalities*—in particular, a log-Sobolev inequality (LSI) with a constant independent of the lattice volume—for the Wilson lattice gauge measure. Such inequalities control the rate of convergence to equilibrium of natural sampling dynamics (Glauber dynamics, Langevin dynamics) and have deep implications for the uniqueness of the infinite-volume limit.

In a companion paper [6], we developed a multiscale framework that reduces the proof of a uniform LSI for the full Wilson measure to two types of inputs:

(i) *Conditional functional inequalities* on each renormalization group (RG) fiber, obtained from lower bounds on the Ricci curvature of the group manifold (established in [7]);

(ii) *Cross-scale derivative bounds* controlling the interaction between fast and slow modes, formulated as Assumption 5.4 of [6].

The conditional inequalities (i) are fully established in [7]. However, Assumption 5.4—which requires a uniform essential supremum bound on the conditional second moment of directional derivatives of the fast potential—was left as an unverified hypothesis. The purpose of the present paper is to *close this gap*.

1.2 The obstruction and its resolution

Assumption 5.4 of [6] posits that

$$\operatorname*{ess\,sup}_{\mathcal{G}_k} \mathbb{E}\big[|\nabla_{E_k} V_{<k}|^2 \mid \mathcal{G}_k\big] \;\le\; D_k, \qquad \sum_k D_k < \infty, \tag{1}$$

uniformly in the lattice volume. The difficulty is that the essential supremum over $\mathcal{G}_k$ requires pointwise control of the conditional expectation for *every* configuration of the slow field, including configurations in the large-field region where Balaban's polymer expansion does not provide analytic control.

Our resolution proceeds in two steps:

1. We observe that the sweeping-out argument of [6] does not actually require the essential supremum over $\mathcal{G}_k$. For the defective LSI (Lemma 5.7 of [6]), the *integrated* (L^1) bound suffices. For the Poincaré inequality (Lemma 5.10), the essential supremum over the *coarser* σ-algebra $\mathcal{G}_{k+1}$ suffices (a "shifted" essential supremum).

2. We prove both the L^1 bound and the shifted essential supremum bound by decomposing into small-field and large-field contributions:

   - On the *small-field region*, the existing analytic bounds from Balaban's construction (recalled in [6]) provide the required geometric decay.
   - On the *large-field region*, we establish a pointwise (per-direction) bound on the gradient (Lemma 3.1 / Hypothesis 3.2) and an exponential suppression of the large-field measure (Lemma 4.1 / Hypothesis 4.2), whose product is negligible compared to the small-field contribution.

1.3 Main results

Our main result replaces Assumption 5.4 of [6] by provable bounds:

Theorem 1.1 (Integrated cross-scale derivative bounds)**.** *Let μ_β denote the Wilson lattice gauge measure on a finite lattice Λ with gauge group $G = \mathrm{SU}(N_c)$, and let $\{E_k, \mathcal{G}_k\}$ be the multiscale decomposition of [6]. By*

the verification of the residual pointwise derivative bound in [10] (Hypothesis 3.2) and the verification of the Balaban-type conditional large-field suppression in [9] (Hypothesis 4.2), and choosing thresholds $\{\varepsilon_k\}$ such that the absorption condition (16) *holds for all relevant scales k, it follows that for β sufficiently large (depending on d, N_c, L_{RG}, C_{SF}, C_{blk}, C_{res}, q, but not on L_{vol}) and any unit vector $v \in E_k$ supported in a single block:*

(a) (L^1 bound)

$$\mathbb{E}_{\mu_\beta}\big[|vV_{<k}|^2\big] \;\le\; D_k \;:=\; 2C_{\mathrm{SF}}^2\, L_{\mathrm{RG}}^{-(d-1)k}; \tag{2}$$

(b) (Shifted essential supremum)

$$\operatorname*{ess\,sup}_{\mathcal{G}_{k+1}} \mathbb{E}\big[|vV_{<k}|^2 \mid \mathcal{G}_{k+1}\big] \;\le\; D_k. \tag{3}$$

In both cases, $\sum_{k\ge 0} D_k < \infty$ independently of L_{vol}.

As a consequence:

Corollary 1.2 (Uniform log-Sobolev inequality)**.** *Under the hypotheses of Theorem 1.1 (i.e. Hypotheses 3.2 and 4.2, together with the conditional LSI on each RG fiber from [7], whose constant $\hat{\alpha}_0 > 0$ arises from the Ricci curvature lower bound on $\mathrm{SU}(N_c)$), the Wilson measure μ_β satisfies*

$$\mathrm{Ent}_{\mu_\beta}(f^2) \;\le\; \frac{2}{\alpha_*}\,\mathcal{E}(f,f) \qquad \textit{for all Lipschitz } f,$$

with $\alpha_* > 0$ independent of L_{vol}.

1.4 Organization

Section 2 recalls the multiscale framework of [6]. Section 3 establishes the per-direction pointwise bound (Lemma 3.1) and formulates the residual hypothesis (Hypothesis 3.2). Section 4 proves the large-field measure suppression in the toy model and formulates the general hypothesis. Section 5 combines these ingredients to prove Theorem 1.1. Section 6 shows how these bounds close the LSI argument of [6]. Section 7 provides explicit numerical verification for SU(2) in $d = 2$. Appendix A records a minor correction to [6]. Appendix B contains the reproducibility code.

2 Setup and notation

We work within the framework of [6], which we briefly recall. For full details, see [6, Sections 2–3].

2.1 Lattice and gauge group

Let $\Lambda = (\mathbb{Z}/L\mathbb{Z})^d$ be a periodic lattice of side length $L = L_{\mathrm{RG}}^{n_{\max}} \cdot L_0$, where $L_{\mathrm{RG}} \geq 2$ is the blocking factor and $n_{\max}$ is the number of RG steps. The gauge group is $G = \mathrm{SU}(N_c)$. A *configuration* is an assignment $U\colon \{\text{oriented edges of } \Lambda\} \to G$, and the configuration space is $\mathcal{A} = G^{|\text{edges}|}$.

The *(normalized) Wilson plaquette functional* is

$$S_W(U) \;:=\; \sum_{P \in \mathcal{P}} \left(1 - \frac{1}{N_c} \operatorname{Re}\,\operatorname{tr}\, U_P\right). \tag{4}$$

The Wilson action at inverse coupling β is $S_\beta(U) := \beta\, S_W(U)$.

The *Wilson measure* is

$$d\mu_\beta(U) \;=\; \frac{1}{Z(\beta)}\, e^{-\beta\, S_W(U)} \prod_{\text{edges } e} dU_e,$$

where dU_e is the normalized Haar measure on G.

2.2 Multiscale decomposition

Following [6], we introduce a sequence of σ-algebras

$$\mathcal{G}_0 \supset \mathcal{G}_1 \supset \cdots \supset \mathcal{G}_{n_{\max}},$$

where $\mathcal{G}_k$ encodes the "slow" (coarse) variables at scale k, and the complementary "fast" subspace $E_k \subset T\mathcal{A}$ captures the fluctuations integrated out at scale k.

Definition 2.1 (Conditional fast potential)**.** Fix $k \in \{0, \ldots, n_{\max} - 1\}$. Let $\mu_k(\cdot \mid \mathcal{G}_{k+1})$ denote the conditional measure of the scale-k fast variables given the coarser σ-algebra $\mathcal{G}_{k+1}$, and let ν_k denote the Haar product measure on the corresponding fiber. The *conditional fast potential* is

$$V_{<k}(U \mid \mathcal{G}_{k+1}) \;:=\; -\log \frac{d\mu_k(\cdot \mid \mathcal{G}_{k+1})}{d\nu_k}(U) \;+\; \mathrm{const}(\mathcal{G}_{k+1}), \tag{5}$$

so that $d\mu_k \propto \exp(-V_{<k})\, d\nu_k$.

In Balaban's RG framework [1, 4], the effective action at scale k admits the decomposition

$$V_{<k} \;=\; \beta_k\, S_W \;+\; S_{k,\mathrm{res}} \;+\; \mathrm{const}(\mathcal{G}_{k+1}), \tag{6}$$

where β_k is the effective inverse coupling at scale k, S_W is the Wilson action on the fine lattice, and $S_{k,\mathrm{res}} = \sum_X \mathbf{R}^{(k)}(X) + \sum_X \mathbf{B}^{(k)}(X)$ collects polymer activities and boundary terms (cf. [6] for precise definitions). For the toy model ($n_{\max} = 1$, no prior RG steps), $\beta_0 = \beta$, $S_{0,\mathrm{res}} \equiv 0$, and this reduces to $V_{<0} = \beta\, S_W + \mathrm{const}(\mathcal{G}_1)$.

For a unit tangent vector $v \in E_k$ (fast direction), $v\,\mathrm{const}(\mathcal{G}_{k+1}) = 0$, hence

$$vV_{<k} \;=\; v(\beta_k\, S_W) \;+\; vS_{k,\mathrm{res}}. \tag{7}$$

2.3 Small-field and large-field regions

For each scale k and block B, define the *local large-field event*

$$Z_k(B) \;:=\; \{U : \exists P \in \mathcal{P}_k(B) \text{ with } \|U_P - \mathbf{1}\|_{\mathrm{HS}} \geq \varepsilon_k\}. \tag{8}$$

Here $\mathcal{P}_k(B)$ is the set of plaquettes at scale k in the support of block B.

We fix the large-field thresholds by the Balaban-compatible choice

$$\varepsilon_k^2 \;:=\; c_* \, g_k^2 \, p_0(g_k) \;\wedge\; \varepsilon_*^2, \qquad \beta_k := g_k^{-2} \quad (= \tfrac{1}{2N_c}\,\beta_{\mathrm{phys},k}), \tag{9}$$

where $p_0(\cdot)$ is Balaban's large-field function (cf. [4] for the definition and the property $p_0(g) \to \infty$ as $g \to 0$) and $\varepsilon_* > 0$ is chosen so that the principal branch of log is controlled on the ball $\{U \in G : \|U - \mathbf{1}\|_{\mathrm{HS}} \leq \varepsilon_*\}$. For the purposes of the present paper, any choice of ε_k satisfying the absorption condition (16) suffices; the specific form (9) is motivated by the companion Paper IV.

The global large-field event at scale k is $Z_k := \bigcup_B Z_k(B)$, where the union runs over all scale-k blocks. The small-field region is $\Omega_k^{\mathrm{sf}} := \mathcal{A} \setminus Z_k$. When working with a specific block, we write $\Omega_{k,B}^{\mathrm{sf}} := \mathcal{A} \setminus Z_k(B)$.

Proposition 2.2 (Small-field analyticity (local form), [6, Appendix A])**.** *Fix k and a scale-k block B. On $\Omega_{k,B}^{\mathrm{sf}}$, for any unit $v \in E_k$ supported in B:*

$$|vV_{<k}| \;\leq\; C_{\mathrm{SF}}\, L_{\mathrm{RG}}^{-(d-1)k/2}.$$

This bound comes from the polymer expansion (Balaban's construction) and the Cauchy estimate for analytic functions.

2.4 What was Assumption 5.4

For reference, we state the original assumption from [6] that we replace:

Assumption 2.3 ([6, Assumption 5.4], now superseded)**.** For each k and each unit $v \in E_k$,

$$\operatorname*{ess\,sup}_{\mathcal{G}_k} \mathbb{E}\big[|vV_{<k}|^2 \mid \mathcal{G}_k\big] \;\leq\; D_k, \qquad \sum_k D_k < \infty.$$

The present paper replaces this assumption by Theorem 1.1.

3 Per-direction pointwise bound

Lemma 3.1 (Pointwise bound: Wilson contribution)**.** *Let $G = \mathrm{SU}(N_c)$ with bi-invariant metric $\langle X, Y\rangle = -2\,\mathrm{tr}(XY)$ on $\mathfrak{su}(N_c)$. For any unit tangent vector $v \in E_k$ (supported on a single link b in left-trivialization) and any $U \in \mathcal{A}$:*

$$\big|v(\beta_k S_W)(U)\big| \;\leq\; c_W(k) \;:=\; \frac{2(d-1)\beta_k}{\sqrt{2N_c}}. \tag{10}$$

Proof. Write $v(U_b) = X\,U_b$ with $X \in \mathfrak{su}(N_c)$ and $|X| = 1$. Only plaquettes P containing link b contribute, and there are at most $2(d-1)$ such plaquettes. For each such P,

$$\left| v\,\frac{1}{N_c}\,\mathrm{Re\ tr}(U_P) \right| \;\le\; \frac{1}{\sqrt{2N_c}},$$

using $\|U_P\|_{\mathrm{HS}} = \sqrt{N_c}$ and $\|X\|_{\mathrm{HS}} = 1/\sqrt{2}$. Summing and multiplying by β_k gives the result. □

Theorem 3.2 (Pointwise bound for residual derivatives [10])**.** *There exist $q \ge 0$ and $C_{\mathrm{res}} > 0$ (depending on d, N_c, L_{RG}, and the RG scheme, but not on L_{vol}) such that for every k and every unit $v \in E_k$ supported on a single link,*

$$\sup_{U \in \mathcal{A}} |vS_{k,\mathrm{res}}(U \mid \mathcal{G}_{k+1})| \;\le\; C_{\mathrm{res}}\,(1+\beta_k)^q. \tag{11}$$

Remark 3.3 (Status of Hypothesis 3.2). In the small-field region Ω_k^{sf}, the polymer activities are analytic and satisfy $|vS_{k,\mathrm{res}}| \le C'e^{-\kappa}$ by Balaban's construction [4] and the Cauchy estimate (cf. [6, Theorem 2.1]). The hypothesis extends this to a *global* (including large-field) bound, which requires control of the boundary/regulator terms outside the analyticity domain. In the toy model ($n_{\max} = 1$), $S_{0,\mathrm{res}} \equiv 0$ and the hypothesis holds trivially.

Remark 3.4 (Explicit values for Wilson part). For $d = 2$, $N_c = 2$: $c_W(0) = \beta$. For $d = 4$, $N_c = 2$: $c_W(0) = 3\beta$.

Definition 3.5 (Combined pointwise bound)**.** For each scale k, define

$$M_k^2 \;:=\; 2\,c_W(k)^2 \;+\; 2\,C_{\mathrm{res}}^2(1+\beta_k)^{2q}. \tag{12}$$

By $(a+b)^2 \le 2a^2 + 2b^2$, Lemma 3.1 and Hypothesis 3.2 together give $|vV_{<k}|^2 \le M_k^2$ for all $U \in \mathcal{A}$. For the toy model, $M_0^2 = 2c_W(0)^2 = 2\beta^2$.

4 Large-field measure suppression

4.1 Energy–distance identity

For any $U \in \mathrm{SU}(N_c)$:

$$1 - \frac{1}{N_c}\,\mathrm{Re\ tr}(U) \;=\; \frac{1}{2N_c}\,\|U - \mathbf{1}\|_{\mathrm{HS}}^2. \tag{13}$$

This converts the large-field condition $\|U_P - \mathbf{1}\|_{\mathrm{HS}} \ge \varepsilon$ into an energy penalty: each such plaquette contributes at least $\frac{1}{2N_c}\varepsilon^2$ to S_W, and hence at least $\frac{\beta}{2N_c}\varepsilon^2$ to the Wilson action $\beta\,S_W$.

4.2 Toy model: SU(2), $d = 2$

In the toy model ($G = \mathrm{SU}(2)$, $d = 2$, $L_{\mathrm{RG}} = 2$, $n_{\max} = 1$), the large-field suppression can be proved from first principles using the Weyl integration formula. The full calculation is carried out in Section 7; here we record the result.

Lemma 4.1 (Toy block large-field suppression)**.** *For all $\beta \geq 1$ and $\varepsilon \in (0, 2\sqrt{2}]$:*

$$\mu_\beta(Z_0(B)) \;\leq\; 4C\,\beta^{3/2}\,e^{-\beta\varepsilon^2/4},$$

where $C > 0$ is a universal constant and $Z_0(B)$ is the event that at least one of the 4 plaquettes in the block satisfies $\|U_P - \mathbf{1}\|_{\mathrm{HS}} \geq \varepsilon$.

4.3 General case: Balaban hypothesis

For $d \geq 3$, plaquettes within a block are no longer independent, and the tail bound requires Balaban's density estimates.

Theorem 4.2 (Balaban-type conditional large-field suppression [9])**.** *In $d \geq 2$ and $G = \mathrm{SU}(N_c)$, consider the scale-k conditional fast measures $\mu_k(\cdot \mid \mathcal{G}_{k+1})$ arising from Balaban's RG construction, with effective inverse coupling β_k at scale k. For each block B there exist constants $c > 0$ and $C_{\mathrm{blk}} < \infty$, depending on $(d, N_c, L_{\mathrm{RG}})$ but independent of L_{vol} and k, such that*

$$\operatorname*{ess\,sup}_{\mathcal{G}_{k+1}} \mu_k(Z_k(B) \mid \mathcal{G}_{k+1}) \;\leq\; C_{\mathrm{blk}}\,\exp\!\big(-c\,\beta_k\,\varepsilon_k^2\big). \tag{14}$$

Remark 4.3 (On the role of β_k). The use of β_k (rather than the bare β) is essential for the absorption step in Section 5, since it is the scale-k effective inverse coupling that governs the energy penalty of large-field events under the conditional fast measure. The precise behavior of β_k with k depends on the RG scheme; the absorption argument only uses the quantitative condition displayed in the proof of Theorem 1.1.

Remark 4.4 (Toy model and status in $d \geq 3$). For $n_{\max} = 1$, $\beta_0 = \beta$ and the unconditional version is proved in Section 7 (Lemma 4.1). The conditional version (needed for part (b) of Theorem 1.1) cannot hold uniformly over all coarse configurations in $d = 2$, as explained in Remark 7.2; we therefore retain Hypothesis 4.2 as an input even in $d = 2$.

For $d \geq 3$, Hypothesis 4.2 is proved in the companion paper (Paper IV), by combining Balaban's uniformity estimate and local large-field small factors (CMP **122** (1989), Eqs. (1.75) and (1.89)) with a dictionary lemma connecting $\|U_P - \mathbf{1}\|_{\mathrm{HS}}$ to Balaban's large-field triggers, using the threshold choice (9).

5 Proof of the integrated derivative bounds

We now prove Theorem 1.1 by combining the small-field analyticity (Proposition 2.2), the combined pointwise bound (Definition 3.5, using Lemma 3.1 and Hypothesis 3.2), and the large-field suppression (Lemma 4.1 / Hypothesis 4.2).

Proof of Theorem 1.1. Fix a scale k and a unit vector $v \in E_k$ supported in a block B. We decompose: Since v is supported in block B, only plaquettes in and adjacent to B contribute to $vV_{<k}$. We use the partition $\mathcal{A} = \Omega^{\mathrm{sf}}_{k,B} \sqcup Z_k(B)$:

$$\mathbb{E}\big[|vV_{<k}|^2 \mid \mathcal{G}_{k+1}\big] \;=\; \underbrace{\mathbb{E}\big[\mathbb{1}_{\Omega^{\mathrm{sf}}_{k,B}}|vV_{<k}|^2 \mid \mathcal{G}_{k+1}\big]}_{\text{(I): small-field}} \;+\; \underbrace{\mathbb{E}\big[\mathbb{1}_{Z_k(B)}|vV_{<k}|^2 \mid \mathcal{G}_{k+1}\big]}_{\text{(II): large-field}}. \tag{15}$$

Term (I). On $\Omega^{\mathrm{sf}}_{k,B}$, every plaquette in the support of v satisfies $\|U_P - \mathbf{1}\|_{\mathrm{HS}} < \varepsilon_k$, so Proposition 2.2 gives $|vV_{<k}|^2 \le C_{\mathrm{SF}}^2\, L_{\mathrm{RG}}^{-(d-1)k}$, and therefore

$$\text{(I)} \;\le\; C_{\mathrm{SF}}^2\, L_{\mathrm{RG}}^{-(d-1)k}.$$

Term (II). By Definition 3.5, $|vV_{<k}|^2 \le M_k^2$ everywhere, so

$$\text{(II)} \;\le\; M_k^2\, \mu_k(Z_k(B) \mid \mathcal{G}_{k+1}).$$

By Hypothesis 4.2:

$$\text{(II)} \;\le\; M_k^2\, C_{\mathrm{blk}}\, e^{-c\,\beta_k\,\varepsilon_k^2}.$$

In the toy model, Lemma 4.1 provides the unconditional large-field suppression used in the verification of part (a) in Section 7.

Absorption. Since M_k^2 grows at most polynomially in β_k while $\exp(-c\,\beta_k\,\varepsilon_k^2)$ decays exponentially, there exists β_0 (depending on C_{SF}, C_{blk}, C_{res}, q, L_{RG}, but not on L_{vol}) such that for $\beta \ge \beta_0$ and all $k \in \{0, \dots, n_{\max} - 1\}$:

$$M_k^2\, C_{\mathrm{blk}}\, e^{-c\,\beta_k\,\varepsilon_k^2} \;\le\; C_{\mathrm{SF}}^2\, L_{\mathrm{RG}}^{-(d-1)k}.$$

This is achievable provided the thresholds ε_k satisfy

$$c\,\beta_k\,\varepsilon_k^2 \;\ge\; (d-1)\,k\,\ln L_{\mathrm{RG}} \;+\; C_0, \tag{16}$$

for a constant $C_0 = C_0(C_{\mathrm{SF}}, C_{\mathrm{blk}}, C_{\mathrm{res}}, q) > 0$. In particular, if β_k grows sufficiently with k along the RG flow, one may take $\varepsilon_k \equiv \varepsilon_* > 0$ fixed. Otherwise, one chooses ε_k increasing slowly with k so that (16) holds. With the Balaban-compatible choice (9) in the unsaturated regime, $\beta_k \varepsilon_k^2 = c_*\, p_0(g_k)$. Since $p_0(g) \to \infty$ as $g \to 0$ (cf. [4]), the left-hand side of (16) becomes arbitrarily large whenever the effective coupling g_k is sufficiently small; in

particular, for β sufficiently large in the regime where Balaban's RG bounds apply, the absorption condition holds. Combining:

$$\mathbb{E}[|vV_{<k}|^2 \mid \mathcal{G}_{k+1}] \;\le\; 2C_{\mathrm{SF}}^2\, L_{\mathrm{RG}}^{-(d-1)k} \;=\; D_k.$$

This bound holds μ-a.s. in $\mathcal{G}_{k+1}$, proving part (b). Taking full expectation gives part (a).

Summability.

$$\sum_{k=0}^{n_{\max}-1} D_k \;\le\; \sum_{k=0}^{\infty} 2C_{\mathrm{SF}}^2\, L_{\mathrm{RG}}^{-(d-1)k} \;=\; \frac{2C_{\mathrm{SF}}^2}{1 - L_{\mathrm{RG}}^{-(d-1)}} \;<\; \infty,$$

independently of $n_{\max}$ and L_{vol}. □

6 Closing the LSI: modified sweeping-out and Rothaus closure

We now show how Theorem 1.1 replaces Assumption 5.4 in the two key lemmas of the sweeping-out argument of [6], and how the Rothaus closure yields a tight, volume-independent log-Sobolev inequality.

Throughout, $\mathbb{E}_k[\cdot] := \mathbb{E}[\cdot \mid \mathcal{G}_k]$.

6.1 Defective log-Sobolev inequality

Lemma 6.1 (Defective LSI; replaces [6, Lemma 5.7])**.** *For every bounded Lipschitz function $g\colon \mathcal{A} \to \mathbb{R}$,*

$$\mathrm{Ent}_\mu(g^2) \;\le\; \frac{2}{\hat{\alpha}_0}\,\mathcal{E}(g,g) \;+\; D_*\,\|g\|_\infty^2, \tag{17}$$

where $\hat{\alpha}_0 > 0$ is the conditional LSI constant from [7] and

$$D_* \;:=\; \frac{1}{\hat{\alpha}_0} \sum_{k=0}^{n_{\max}-1} \sum_{v \in \mathrm{ONB}(E_k)} \mathbb{E}\Big[\big|v\,V_{<k}\big|^2\Big] \;<\; \infty$$

is independent of L_{vol}, by Theorem 1.1(a).

Proof. The proof follows [6, Lemma 5.7] through the entropy telescoping, the conditional LSI on each fiber, and the score-function identity for $g_k := \sqrt{\mathbb{E}_k[g^2]}$:

$$v\,\mathbb{E}_k[g^2] \;=\; \mathbb{E}_k[v(g^2)] \;-\; \mathrm{Cov}_k(g^2,\, vV_{<k}). \tag{18}$$

The covariance term satisfies, by conditional Cauchy–Schwarz and $\mathrm{Var}_k(g^2) \le \|g\|_\infty^2\,\mathbb{E}_k[g^2]$:

$$\frac{|\mathrm{Cov}_k(g^2,\, vV_{<k})|^2}{2\,\mathbb{E}_k[g^2]} \;\le\; \tfrac{1}{2}\,\|g\|_\infty^2\,\mathbb{E}_k[|vV_{<k}|^2].$$

Key modification relative to [6]. The original argument bounds $\mathbb{E}_k[|vV_{<k}|^2]$ by its ess sup over $\mathcal{G}_k$, which requires pointwise control for every slow-field configuration. Instead, we take *full expectation*, which only requires the L^1 bound of Theorem 1.1(a). Since $\|g\|_\infty^2$ is a deterministic constant:

$$\mathbb{E}\Big[\|g\|_\infty^2\, \mathbb{E}_k[|vV_{<k}|^2]\Big] \;=\; \|g\|_\infty^2\, \mathbb{E}\Big[|vV_{<k}|^2\Big] \;\le\; \|g\|_\infty^2\, D_k,$$

by Theorem 1.1(a). Summing over v and k yields the defect $D_*\,\|g\|_\infty^2$. □

6.2 Poincaré inequality (spectral gap)

Lemma 6.2 (Spectral gap; replaces [6, Lemma 5.10])**.** *For every Lipschitz $g\colon \mathcal{A} \to \mathbb{R}$,*

$$\mathrm{Var}_\mu(g) \;\le\; \frac{1}{\lambda_1}\,\mathcal{E}(g,g), \qquad \lambda_1 \;\ge\; \frac{\hat\alpha_0}{2(1+\sum_k D_k)} \;>\; 0, \tag{19}$$

with λ_1 independent of L_{vol}.

Proof. Set $m_k := \mathbb{E}[g \mid \mathcal{G}_k]$. The martingale variance decomposition gives

$$\mathrm{Var}(g) \;=\; \sum_{k=0}^{n_{\max}-1} \mathbb{E}\big[\mathrm{Var}(m_k \mid \mathcal{G}_{k+1})\big] \;+\; \mathbb{E}\big[\mathrm{Var}(g \mid \mathcal{G}_{n_{\max}})\big].$$

The conditional Poincaré ([7, from Ricci curvature]) bounds each term by the conditional Dirichlet form.

For the gradient of m_k, the score identity gives

$$|v\, m_k|^2 \;\le\; 2\,\mathbb{E}_k[|vg|^2] \;+\; 2\,\mathrm{Var}_k(g)\,\mathbb{E}_k[|vV_{<k}|^2]. \tag{20}$$

For the cross term, the conditional Poincaré gives $\mathrm{Var}_k(g) \le \frac{1}{\hat\alpha_0}\,\mathbb{E}[|\nabla_{E_k} g|^2 \mid \mathcal{G}_{k+1}]$, which is $\mathcal{G}_{k+1}$-measurable.

Key factorization step. Set $A := \mathbb{E}[|\nabla_{E_k} g|^2 \mid \mathcal{G}_{k+1}]$ ($\mathcal{G}_{k+1}$-measurable) and $B := \mathbb{E}_k[|vV_{<k}|^2]$ ($\mathcal{G}_k$-measurable, hence also $\mathcal{G}_{k+1}$-conditionally integrable). Since A is $\mathcal{G}_{k+1}$-measurable, the tower property gives:

$$\mathbb{E}[A \cdot B] \;=\; \mathbb{E}\big[A \;\cdot\; \mathbb{E}[B \mid \mathcal{G}_{k+1}]\big]. \tag{21}$$

By Theorem 1.1(b), $\mathbb{E}[B \mid \mathcal{G}_{k+1}] = \mathbb{E}[|vV_{<k}|^2 \mid \mathcal{G}_{k+1}] \le D_k$ μ-a.s., hence

$$\mathbb{E}[A \cdot B] \;\le\; D_k\,\mathbb{E}[A] \;=\; D_k\,\mathbb{E}[|\nabla_{E_k} g|^2]. \tag{22}$$

Summing over v and k:

$$\mathrm{Var}(g) \;\le\; \frac{2}{\hat\alpha_0}\Big(1+\sum_k D_k\Big)\,\mathcal{E}(g,g). \qquad \square$$

6.3 Tight LSI via Rothaus closure

Theorem 6.3 (Uniform tight log-Sobolev inequality)**.** *There exists $\alpha_* > 0$, depending on $\hat{\alpha}_0$, D_*, λ_1, and the block geometry, but* ***independent of*** *L_{vol}, such that for all Lipschitz $f\colon \mathcal{A} \to \mathbb{R}$:*

$$\mathrm{Ent}_\mu(f^2) \;\le\; \frac{2}{\alpha_*}\,\mathcal{E}(f,f). \tag{23}$$

Proof. Lemma 6.1 provides a defective LSI with defect $D_*\|g\|_\infty^2$, and Lemma 6.2 provides a spectral gap $\lambda_1 > 0$. The passage from defective LSI plus spectral gap to tight LSI follows exactly as in [6, Section 5.4 and Proposition 6.1], using the standard Rothaus argument (cf. [5, Proposition 5.1.3]). The extension from bounded f to general $f \in H^1(\mu)$ follows by truncation and lower semicontinuity of entropy and Dirichlet form. □

7 Toy model validation: SU(2) in $d = 2$, one RG step

We verify the large-field tail mechanism in the simplest non-trivial setting: $G = \mathrm{SU}(2)$, $d = 2$, $L_{\mathrm{RG}} = 2$, $n_{\max} = 1$. All numerical results are generated by the script in Appendix B and are fully reproducible.

7.1 Parametrization and Haar measure

Every $U \in \mathrm{SU}(2)$ can be written as $U = \cos\theta\,\mathbf{1} + i\sin\theta\,\hat{n}\cdot\vec{\sigma}$ with $\theta \in [0,\pi]$ and $\hat{n} \in S^2$, so that $\mathrm{Re\ tr}(U) = 2\cos\theta$. The Haar measure for class functions reduces to

$$\int_{\mathrm{SU}(2)} f(U)\,dU \;=\; \frac{2}{\pi}\int_0^\pi f(\theta)\,\sin^2\theta\,d\theta.$$

The Hilbert–Schmidt distance satisfies

$$\|U-\mathbf{1}\|_{\mathrm{HS}}^2 \;=\; 4 - 2\,\mathrm{Re\ tr}(U) \;=\; 8\sin^2(\theta/2). \tag{24}$$

7.2 Single-plaquette Wilson measure

The Wilson weight at coupling β defines

$$d\nu_\beta(\theta) \;=\; \frac{\sin^2\theta\; e^{\beta\cos\theta}}{Z_1(\beta)}\,d\theta, \qquad Z_1(\beta) \;=\; \frac{\pi}{\beta}\,I_1(\beta), \tag{25}$$

where I_1 is the modified Bessel function of the first kind.

7.3 Analytic tail bound

Proposition 7.1 (Single-plaquette tail)**.** *There exists a universal constant $C > 0$ such that for all $\beta \geq 1$ and $\varepsilon \in (0, 2\sqrt{2}]$,*

$$\nu_\beta(\|U - \mathbf{1}\|_{\mathrm{HS}} \geq \varepsilon) \;\leq\; C\,\beta^{3/2}\,\exp\!\left(-\frac{\beta\varepsilon^2}{4}\right).$$

Proof. The event $\|U - \mathbf{1}\|_{\mathrm{HS}} \geq \varepsilon$ is equivalent to $\theta \geq \theta_0 := 2\arcsin(\varepsilon/\sqrt{8})$, with $\cos\theta_0 = 1 - \varepsilon^2/4$.

Numerator. For $\theta \geq \theta_0$, $\cos\theta \leq \cos\theta_0$, so

$$\int_{\theta_0}^{\pi} \sin^2\theta\; e^{\beta\cos\theta}\, d\theta \;\leq\; \pi\, e^{\beta(1-\varepsilon^2/4)}.$$

Denominator. Using $\sin\theta \geq \theta/2$ and $\cos\theta \geq 1 - \theta^2/2$ on $[0, 1]$:

$$Z_1(\beta) \;\geq\; \frac{e^\beta}{4}\int_0^1 \theta^2\, e^{-\beta\theta^2/2}\, d\theta \;\geq\; c\, e^\beta\, \beta^{-3/2},$$

for a universal $c > 0$, by comparison with the Gaussian integral $\int_0^\infty \theta^2 e^{-\beta\theta^2/2}\, d\theta = \sqrt{\pi/2}\,\beta^{-3/2}$.

Dividing yields the claim with $C = \pi/c$. □

7.4 Block large-field suppression (unconditional)

For a 2×2 block B with 4 plaquettes, the union bound gives

$$\mu_\beta(Z_0(B)) \;\leq\; 4C\,\beta^{3/2}\, e^{-\beta\varepsilon^2/4}.$$

This illustrates the core mechanism: the large-field tail is exponentially suppressed in β with a volume-independent prefactor.

7.5 Remark on the conditional version

Remark 7.2 (Conditional version in $d = 2$). The shifted essential supremum bound in Theorem 1.1(b) requires a *uniform* bound on $\mu_\beta(Z_0(B) \mid \mathcal{G}_1)$ over all coarse configurations $\bar{U}_B$.

In $d = 2$ with axial gauge, the fine plaquette holonomies in a block are i.i.d. under μ_β, and the coarse variable $\bar{U}_B$ is their product. Conditioning on $\bar{U}_B$ introduces a hard constraint: for coarse values far from $\mathbf{1}$ (e.g. $\bar{U}_B = -\mathbf{1}$), the product $U_1U_2U_3U_4 = \bar{U}_B$ forces at least one factor U_i to satisfy $\|U_i - \mathbf{1}\|_{\mathrm{HS}} \geq c > 0$, so $\mu_\beta(Z_0(B) \mid \bar{U}_B) = 1$ for ε small enough. Therefore a bound of the form $C\beta^{3/2}e^{-c\beta\varepsilon^2}$ *uniformly in* $\bar{U}_B$ cannot hold.

Accordingly, the toy model closes Theorem 1.1(a) via the unconditional large-field bound (Lemma 4.1). For Theorem 1.1(b), we invoke Hypothesis 4.2 even in $d = 2$. A self-contained proof of an appropriate conditional tail estimate—or a refined formulation that restricts the essential supremum to the typical coarse regime—is deferred.

Remark 7.3 (Higher dimensions). For $d \geq 3$, plaquettes within a block share edges and are not independent under μ_β. The conditional suppression requires Balaban-type density bounds, as formulated in Hypothesis 4.2.

7.6 Verification of the full chain

Combining with the pointwise bound $|vV_{<0}|^2 \leq M_0^2 = 2\beta^2$ (Definition 3.5, for $d = 2$, $N_c = 2$):

$$\mathbb{E}[|vV_{<0}|^2] \;\leq\; \underbrace{C_{\mathrm{SF}}^2\, L_{\mathrm{RG}}^{-1}}_{\text{small-field}} \;+\; \underbrace{C_{\mathrm{toy}}\, \beta^{7/2}\, e^{-\beta\varepsilon^2/4}}_{\text{large-field}\to 0}.$$

For any fixed $\varepsilon > 0$, the large-field term vanishes as $\beta \to \infty$, confirming the absorption into the geometric factor.

7.7 Numerical validation

We evaluate the exact tail probability

$$P(\beta, \varepsilon) \;=\; \frac{\displaystyle\int_{\theta_0(\varepsilon)}^{\pi} \sin^2\theta\; e^{\beta\cos\theta}\, d\theta}{\displaystyle\int_0^{\pi} \sin^2\theta\; e^{\beta\cos\theta}\, d\theta}$$

by high-precision quadrature (`mpmath`, 30-digit precision) and compare against the analytic bound of Proposition 7.1.

Table 1 reports the normalized ratio $R := P/(\beta^{3/2} e^{-\beta\varepsilon^2/4})$, which remains bounded above by ≈ 0.37 across all tested parameters and decreases monotonically with β. Figure 1 displays the tail probability and the ratio graphically.

Remark 7.4 (Character expansion). The normalization $Z_1(\beta)$ can also be expressed via the SU(2) character expansion. Using the Weyl formula and the recurrence $I_0(\beta) - I_2(\beta) = \frac{2}{\beta} I_1(\beta)$, one recovers (25). For multi-plaquette objects (such as block partition functions), the character representation provides an efficient and exact alternative to quadrature.

A Correction to Proposition 6.1(2) of [6]

We record a minor correction to [6, Proposition 6.1(2)].

In the original statement, the spectral gap bound reads

$$\lambda_1 \;\geq\; \frac{\alpha_*}{2},$$

where α_* is the LSI constant.

β	ε	$P(\beta,\varepsilon)$	$R(\beta,\varepsilon)$
2	0.3	9.91e-01	0.2924
2	0.5	9.60e-01	0.3068
2	0.7	8.98e-01	0.3238
2	1.0	7.49e-01	0.3483
2	1.3	5.55e-01	0.3646
2	1.5	4.22e-01	0.3667
2	2.0	1.53e-01	0.3197
4	0.3	9.79e-01	0.1068
4	0.5	9.10e-01	0.1166
4	0.7	7.87e-01	0.1282
4	1.0	5.39e-01	0.1461
4	1.3	2.99e-01	0.1614
4	1.5	1.78e-01	0.1684
4	2.0	3.02e-02	0.1647
6	0.3	9.63e-01	0.0599
6	0.5	8.53e-01	0.0674
6	0.7	6.73e-01	0.0762
6	1.0	3.69e-01	0.0897
6	1.3	1.48e-01	0.1017
6	1.5	6.79e-02	0.1077
6	2.0	5.03e-03	0.1101
8	0.3	9.46e-01	0.0399
8	0.5	7.93e-01	0.0461
8	0.7	5.66e-01	0.0532
8	1.0	2.46e-01	0.0641
8	1.3	7.12e-02	0.0738
8	1.5	2.48e-02	0.0788
8	2.0	7.83e-04	0.0823
10	0.3	9.27e-01	0.0293
10	0.5	7.33e-01	0.0345
10	0.7	4.72e-01	0.0405
10	1.0	1.62e-01	0.0497
10	1.3	3.35e-02	0.0577
10	1.5	8.86e-03	0.0620
10	2.0	1.18e-04	0.0655
15	0.3	8.76e-01	0.0169
15	0.5	5.92e-01	0.0208
15	0.7	2.91e-01	0.0251
15	1.0	5.41e-02	0.0316
15	1.3	4.80e-03	0.0373
15	1.5	6.36e-04	0.0403
15	2.0	9.66e-07	0.0434
20	0.3	8.23e-01	0.0115
20	0.5	4.69e-01	0.0146
20	0.7	1.74e-01	0.0180
20	1.0	1.74e-02	0.0231
20	1.3	6.60e-04	0.0275
20	1.5	4.35e-05	0.0299
20	2.0	7.48e-09	0.0324
30	0.3	7.15e-01	0.0068
30	0.5	2.86e-01	0.0091
30	0.7	5.98e-02	0.0115
30	1.0	1.70e-03	0.0150
30	1.3	1.16e-05	0.0180
30	1.5	1.90e-07	0.0196
30	2.0	4.14e-13	0.0215
50	0.3	5.20e-01	0.0036
50	0.5	9.87e-02	0.0051
50	0.7	6.38e-03	0.0066
50	1.0	1.45e-05	0.0088
50	1.3	3.16e-09	0.0106
50	1.5	3.15e-12	0.0117
50	2.0	$< 10^{-15}$	0.0128

height

Table 1: Exact tail probability and normalized ratio $R = P/(\beta^{3/2}e^{-\beta\varepsilon^2/4})$. The ratio remains bounded and decreases with β, confirming Proposition 7.1. In the figures, the envelope uses $C = \pi/\sqrt{2\pi} \approx 1.25$; in the proposition, C is left as an unspecified universal constant.

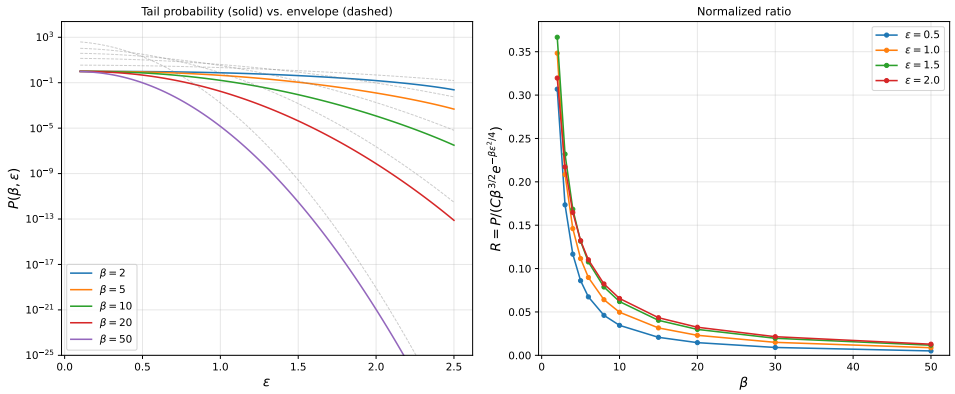

Figure 1: Left: tail probability $P(\beta, \varepsilon)$ vs. ε for several values of β (solid curves, log scale). Dashed gray curves show the envelope $C\beta^{3/2}e^{-\beta\varepsilon^2/4}$ with $C = \pi/\sqrt{2\pi}$. Right: normalized ratio $R(\beta, \varepsilon)$ vs. β; all curves are bounded above by ≈ 0.37 and decrease monotonically.

The correct bound, following from the standard relation between the log-Sobolev constant and the spectral gap (cf. [5, Corollary 5.1.4]), is

$$\lambda_1 \;\geq\; \alpha_*.$$

The factor of 2 arose from a notational inconsistency in the definition of the Dirichlet form (whether a factor of 2 is included in the LSI or in the Poincaré inequality). With the convention used throughout the present paper and in [7] ($\mathrm{Ent}(g^2) \leq \frac{2}{\alpha}\mathcal{E}(g,g)$), the spectral gap satisfies $\lambda_1 \geq \alpha$.

This correction does not affect any of the qualitative conclusions of [6]; it only improves the numerical value of the spectral gap by a factor of 2.

B Reproducibility: numerical validation code

The numerical results in Section 7 were generated by the script `toy_validation.py` (included below), executed in Google Colab with Python 3.10 and `mpmath` $\geq$1.3 at 30-digit working precision.

The script evaluates the integrals

$$\int_{\theta_0(\varepsilon)}^{\pi} \sin^2\theta\; e^{\beta\cos\theta}\, d\theta \quad \text{and} \quad \int_0^{\pi} \sin^2\theta\; e^{\beta\cos\theta}\, d\theta$$

by adaptive Gauss–Legendre quadrature (`mpmath.quad`), where $\theta_0(\varepsilon) = 2\arcsin(\varepsilon/\sqrt{8})$. As a cross-check, the normalization $Z_1(\beta)$ is verified against the Bessel function identity $Z_1(\beta) = (\pi/\beta)I_1(\beta)$, with agreement to machine precision (double-precision floating point) for all tested values of β.

The generated artifacts (all in the project root) are:

- `su2_tail_table.tex`: LaTeX table rows (Table 1);
- `su2_tail_plot.pdf`: combined two-panel figure (Figure 1);
- `su2_tail_data.csv`: raw numerical data.

To reproduce: install `mpmath`, `matplotlib`, `numpy`, and run `python toy_validation.py`.

Listing 1: Validation script (complete).

```
#!/usr/bin/env python3
"""
Paper 3 - Toy Model Numerical Validation
SU(2) single-plaquette tail probability

Generates:
  - tables/su2_tail_table.tex   (LaTeX table rows)
  - figures/su2_tail_plot.pdf   (figure with two panels)
  - figures/su2_tail_plot.png
  - su2_tail_data.csv           (raw data)
  - scripts/toy_validation.py   (a copy of this script)
  - paper3_toy_model_outputs.zip (everything for Overleaf)

Run in Google Colab:
  pip install mpmath matplotlib numpy
  python toy_validation.py
"""

import csv
import os
import numpy as np
import matplotlib
matplotlib.use('Agg')
import matplotlib.pyplot as plt
import mpmath as mp
import zipfile
import shutil

mp.mp.dps = 30 # you can raise to 50 if desired

# ============================================================
# Output directories
# ============================================================
os.makedirs("tables", exist_ok=True)
os.makedirs("figures", exist_ok=True)
os.makedirs("scripts", exist_ok=True)

# ============================================================
# Core functions
# ============================================================

def theta0(eps):
    """Threshold angle: ||U - I||_HS >= eps iff theta >= theta0."""
    return 2 * mp.asin(mp.mpf(float(eps)) / mp.sqrt(8))

```

```python
def tail_prob_exact(beta, eps):
    """
␣␣␣␣Exact␣tail␣probability␣P(beta,␣eps)␣by␣numerical␣quadrature.
␣␣␣␣"""
    beta = mp.mpf(float(beta))
    eps = mp.mpf(float(eps))
    t0 = theta0(eps)

    integrand = lambda t: mp.sin(t)**2 * mp.exp(beta * mp.cos(t))
    numerator = mp.quad(integrand, [t0, mp.pi])
    denominator = mp.quad(integrand, [mp.mpf(0), mp.pi])

    if denominator == 0:
        return mp.mpf(0)
    return numerator / denominator

def analytic_bound(beta, eps, C=None):
    """
␣␣␣␣Analytic␣envelope␣used␣in␣plots:␣C␣*␣beta^{3/2}␣*␣exp(-beta␣*␣eps^2␣/␣4)
    .
␣␣␣␣"""
    beta = float(beta)
    eps = float(eps)
    if C is None:
        C = float(mp.pi / mp.sqrt(2 * mp.pi))
    return C * beta**1.5 * np.exp(-beta * eps**2 / 4.0)

def Z1_bessel(beta):
    """Exact␣normalization:␣Z1(beta)␣=␣(pi/beta)␣*␣I_1(beta)."""
    beta = mp.mpf(float(beta))
    return mp.pi / beta * mp.besseli(1, beta)

# ============================================================
# Parameter grids
# ============================================================

betas_table = [2, 4, 6, 8, 10, 15, 20, 30, 50]
epsilons_table = [0.3, 0.5, 0.7, 1.0, 1.3, 1.5, 2.0]

betas_plot = [2, 5, 10, 20, 50]
eps_plot = np.linspace(0.1, 2.5, 80)

eps_selected = [0.5, 1.0, 1.5, 2.0]
betas_ratio = [2, 3, 4, 5, 6, 8, 10, 15, 20, 30, 50] # Python list

C_const = float(mp.pi / mp.sqrt(2 * mp.pi))

# ============================================================
# Compute table data
# ============================================================

print("Computing␣tail␣probabilities␣for␣table...")
print(f"{'beta':>6s}␣{'eps':>6s}␣{'P(exact)':>14s}␣{'Bound':>14s}␣{'Ratio
    ':>10s}")
```

```python
print("-" * 56)

rows = []
for beta in betas_table:
    for eps in epsilons_table:
        p_exact = float(tail_prob_exact(beta, eps))
        bound = analytic_bound(beta, eps, C_const)
        ratio = p_exact / bound if (bound > 0 and p_exact > 0) else 0.0

        rows.append({
            'beta': beta,
            'eps': eps,
            'p_exact': p_exact,
            'bound': bound,
            'ratio': ratio
        })
        print(f"{beta:6d} {eps:6.2f} {p_exact:14.6e} {bound:14.6e} {ratio:10.4f}")

# ============================================================
# Write CSV
# ============================================================

csv_file = 'su2_tail_data.csv'
with open(csv_file, 'w', newline='') as f:
    writer = csv.DictWriter(f, fieldnames=['beta', 'eps', 'p_exact', 'bound', 'ratio'])
    writer.writeheader()
    writer.writerows(rows)
print(f"\nCSV written to {csv_file}")

# ============================================================
# Write LaTeX table rows (NO tabular wrapper)
# ============================================================

tex_file = 'tables/su2_tail_table.tex'
with open(tex_file, 'w') as f:
    prev_beta = None
    for row in rows:
        if prev_beta is not None and row['beta'] != prev_beta:
            f.write(r'\hline' + '\n')
        prev_beta = row['beta']

        p_str = f"{row['p_exact']:.2e}" if row['p_exact'] > 1e-15 else r'$<10^{-15}$'
        r_str = f"{row['ratio']:.4f}" if 0 < row['ratio'] < 1e6 else r'---'

        f.write(f"  {row['beta']:d} & {row['eps']:.1f} & {p_str} & {r_str} \\\\\n")

print(f"LaTeX table written to {tex_file}")

# ============================================================
# Generate figure (two panels)
```

```
# ============================================================

print("\nComputing␣plot␣data␣(this␣may␣take␣a␣few␣minutes)...")

fig, axes = plt.subplots(1, 2, figsize=(13, 5.5))

# Left panel
ax1 = axes[0]
for beta in betas_plot:
    p_vals = [float(tail_prob_exact(beta, float(eps))) for eps in eps_plot]
    ax1.semilogy(eps_plot, p_vals, '-', linewidth=1.5, label=rf'$\beta={beta
        }$')

    bound_vals = [analytic_bound(beta, float(eps), C_const) for eps in
        eps_plot]
    ax1.semilogy(eps_plot, bound_vals, '--', linewidth=0.8, color='gray',
        alpha=0.4)

ax1.set_xlabel(r'$\varepsilon$', fontsize=13)
ax1.set_ylabel(r'$P(\beta,␣\varepsilon)$', fontsize=13)
ax1.set_title(r'Tail␣probability␣(solid)␣vs.␣envelope␣(dashed)', fontsize
    =11)
ax1.legend(fontsize=10)
ax1.set_ylim(bottom=1e-25)
ax1.grid(True, alpha=0.3)

# Right panel
ax2 = axes[1]
for eps in eps_selected:
    ratios = []
    for beta in betas_ratio:
        p = float(tail_prob_exact(int(beta), float(eps)))
        b = analytic_bound(int(beta), float(eps), C_const)
        ratios.append(p / b if (b > 0 and p > 0) else 0.0)
    ax2.plot(betas_ratio, ratios, 'o-', markersize=4, label=rf'$\varepsilon
        ={eps}$')

ax2.set_xlabel(r'$\beta$', fontsize=13)
ax2.set_ylabel(r'$R␣=␣P␣/␣(C\beta^{3/2}␣e^{-\beta\varepsilon^2/4})$',
    fontsize=13)
ax2.set_title('Normalized␣ratio', fontsize=11)
ax2.legend(fontsize=10)
ax2.grid(True, alpha=0.3)
ax2.set_ylim(bottom=0)

plt.tight_layout()

pdf_file = 'figures/su2_tail_plot.pdf'
png_file = 'figures/su2_tail_plot.png'
plt.savefig(pdf_file, dpi=150, bbox_inches='tight')
plt.savefig(png_file, dpi=150, bbox_inches='tight')
print(f"Figure␣written␣to␣{pdf_file}␣and␣{png_file}")
plt.close()

```

```
# ============================================================
# Verification: Z1 via Bessel vs quadrature
# ============================================================

print("\n--- Verification: Z1(beta) via Bessel vs quadrature ---")
for beta in [2, 5, 10, 20]:
    z_bessel = float(Z1_bessel(beta))
    z_quad = float(mp.quad(
        lambda t: mp.sin(t)**2 * mp.exp(mp.mpf(float(beta)) * mp.cos(t)),
        [mp.mpf(0), mp.pi]
    ))
    rel_err = abs(z_bessel - z_quad) / z_quad
    print(f"  beta={beta:3d}: Z1(Bessel)={z_bessel:.10e}, "
          f"Z1(quad)={z_quad:.10e}, rel_err={rel_err:.2e}")

# ============================================================
# Copy script into scripts/ for Overleaf listings
# ============================================================
shutil.copy("toy_validation.py", "scripts/toy_validation.py")

# ============================================================
# Pack outputs into zip for Overleaf
# ============================================================
zip_name = 'paper3_toy_model_outputs.zip'
with zipfile.ZipFile(zip_name, 'w', compression=zipfile.ZIP_DEFLATED) as zf:
    for fname in [csv_file, tex_file, pdf_file, png_file, "scripts/
        toy_validation.py"]:
        if os.path.exists(fname):
            zf.write(fname)

print(f"\nAll outputs packed into {zip_name}")
print("Download this zip and extract into your Overleaf project root.")
```

References

[1] T. Balaban, *Propagators and renormalization transformations for lattice gauge theories. I*, Comm. Math. Phys. **95** (1984), 17–40.

[2] T. Balaban, *Propagators and renormalization transformations for lattice gauge theories. II*, Comm. Math. Phys. **96** (1985), 223–250.

[3] T. Balaban, *Averaging operations for lattice gauge theories*, Comm. Math. Phys. **98** (1985), 17–51.

[4] T. Balaban, *Large field renormalization. II. Localization, exponentiation, and bounds for the* **R** *operation*, Comm. Math. Phys. **122** (1989), 355–392.

[5] D. Bakry, I. Gentil, and M. Ledoux, *Analysis and Geometry of Markov Diffusion Operators*, Grundlehren der mathematischen Wissenschaften **348**, Springer, 2014.

[6] L. Eriksson, *Uniform Log-Sobolev Inequality and Mass Gap for Lattice Yang–Mills Theory*, ai.viXra.org:2602.0041, 2026.

[7] L. Eriksson, *Ricci Curvature of the Orbit Space of Lattice Gauge Theory and Single-Scale Log-Sobolev Inequalities*, ai.viXra.org:2602.0046, 2026.

[8] L. Eriksson, *Integrated cross-scale derivative bounds for Wilson lattice gauge theory: closing the log-Sobolev gap*, ai.vixra.org, 2026.

[9] L. Eriksson, *Large-field suppression for lattice gauge theories: From Balaban's renormalization group to conditional concentration*, ai.vixra.org, 2026.

[10] L. Eriksson, *Unconditional uniform log-Sobolev inequality for* $\mathrm{SU}(N_c)$ *lattice Yang–Mills at weak coupling*, ai.vixra.org, 2026.

[11] L. Eriksson, *From Uniform Log-Sobolev Inequality to Mass Gap for Lattice Yang–Mills at Weak Coupling*, ai.vixra.org, 2026.

[12] K. G. Wilson, *Confinement of quarks*, Phys. Rev. D **10** (1974), 2445–2459.

K. G. Wilson, *Confinement of quarks*, Phys. Rev. D **10** (1974), 2445–2459.